Available online at www.sciencedirect.com
ScienceDirect
International Journal of Pharmaceutics 357 (2008) 6–14
INTERNATIONAL JOURNAL OF PHARMACEUTICS
www.elsevier.com/locate/ijpharm

Decomposition of the Telomere-Targeting agent BRACO19 in physiological media results in products with decreased inhibitory potential

S. Taetz [a], T.E. Mürdter [b], J. Zapp [c], S. Boettcher [d], C. Baldes [a], E. Kleideiter [b], K. Piotrowska [b], U.F. Schaefer [a], U. Klotz [b], C.-M. Lehr [a,*]

[a] *Biopharmaceutics and Pharmaceutical Technology, Saarland University, Campus, Building A 4.1, Saarbrücken 66123, Germany*
[b] *Dr. Margarete Fischer-Bosch Institute of Clinical Pharmacology and University of Tübingen, Auerbachstrasse 112, Stuttgart 70376, Germany*
[c] *Pharmaceutical Biology, Saarland University, Campus, Building C 2.2, Saarbrücken 66123, Germany*
[d] *Pharmaceutical and Medicinal Chemistry, Saarland University, Campus, Building C 2.2, Saarbrücken 66123, Germany*

Received 12 November 2007; received in revised form 7 January 2008; accepted 8 January 2008
Available online 20 January 2008

Abstract

The stability of the acridine-based telomere-targeting agent BRACO19, a G-quadruplex stabilizing substance, was tested at different pH, temperature and in different dissolution media. Analysis was performed by HPLC. Decomposition products were examined by LC/MS and NMR. The TRAP assay was used to determine the inhibitory potential of the decomposition products on telomerase activity. The results show that the stability of BRACO19 strongly depends on pH and temperature. Decomposition was fastest at physiological pH and temperature while the type of dissolution medium had no major influence on stability. The most probable mechanism for this decomposition seems to be a hydrolysis of the amide bonds in position 3 and 6 of the acridine ring and/or a deamination of the phenyl ring. The decomposition products showed a reduced inhibitory potential compared to the parent compound BRACO19. The results demonstrate that the preparation of dosage forms and their storage conditions will have an important influence on the stability – and hence biological efficacy – of BRACO19 and related substances.

Keywords: Acridine; Stability; G-quadruplex; Hydrolysis; Deamination; TRAP assay

1. Introduction

During the last years the concept of telomerase inhibition for the treatment of cancer became an area of intensive research. Telomerase is a reverse transcriptase composed of the catalytic subunit human *te*lomerase *r*everse *t*ranscriptase (hTERT) and the template RNA *h*uman *t*elomerase *R*NA (hTR). Its substrates, the telomeres, are located at the ends of each chromosome. Telomeres are repetitive TTAGGG/AATCCC sequences that end in a 3′-$(TTAGGG)_n$ single strand overhang. They form a so-called *t*-loop, a structure stabilized by associated proteins, where the single strand invades the double stranded region. The *t*-loops prevent the chromosome ends from end-to-end fusions and being recognized as damaged DNA. Due to the end replication problem during DNA duplication telomeres erode at each cell cycle until they approach a certain limit. Reaching this limit is an important signal for a cell to enter the state of cellular senescence. Cells that do not stop dividing will experience severe chromosomal damages leading to cell death (apoptosis). Since most malignant cells express telomerase they are able to maintain their telomeres above this limit and therefore escape these pathways (Shay and Wright, 2004; Blackburn, 2005; Pendino et al., 2006). Various telomerase inhibitors have been developed and successfully tested. They either target hTERT, hTR or the telomeres (Shay and Wright, 2006).

Our studies concentrate on the topical treatment of non-small cell lung cancer (NSCLC) via the inhalative route. A search for suitable drug candidates led to the telomere targeting 3,6,9-aminoacridine derivative BRACO19 ((9-[4-(*N*,*N*-dimethylamino)phenylamino]-3,6-bis(3-pyrrolodino-propionamido) acridine; Fig. 1) which acts by G-quadruplex stabilization (Gowan et al., 2002; Piotrowska

* Corresponding author at: Saarland University, Biopharmaceutics and Pharmaceutical Technology, P.O. Box 15 11 50, Saarbrücken 66041, Germany. Tel.: +49 681 302 3039; fax: +49 681 302 4677.
E-mail address: lehr@mx.uni-saarland.de (C.-M. Lehr).

0378-5173/$ – see front matter © 2008 Elsevier B.V. All rights reserved.
doi:10.1016/j.ijpharm.2008.01.026

et al., 2005). G-quadruplexes are planar G-quartet motifs that can form in guanine-rich DNA sequence like the telomeres. These structures interact with the inhibitor via π–π stacking. Positively charged side chains of the inhibitor interact with the negatively charged phosphate DNA backbone and thereby stabilize the G-quadruplex–inhibitor complex. Due to this mechanism telomeres are not able to form their native structure and hence fail to protect the chromosomes (Cuesta et al., 2003; Riou, 2004).

BRACO19 has shown some promising results in studies in tumor cell cultures and mouse xenografts. It was reported that a treatment with BRACO19 not only resulted in telomerase inhibition but also in general telomere dysfunction that led to atypical mitosis and consequently to apoptosis (Burger et al., 2005).

In a previous study we characterized BRACO19 with respect to its biopharmaceutical properties and found it to be a typical class III drug substance with a good aqueous solubility but a very poor permeability across epithelial cell monolayers (Taetz et al., 2006). During these studies we also found that BRACO19 has stability problems when dissolved in aqueous media at physiological pH.

In the present study we examined the influence of pH, temperature and dissolution media on the stability of BRACO19. We have identified potential decomposition products and evaluated whether they can contribute to the inhibitory action of this drug candidate.

2. Materials and methods

2.1. BRACO19

BRACO19 ((9-[4-(*N*,*N*-dimethylamino)phenylamino]-3,6-bis(3-pyrrolidino-propionamido) acridine) × 3HCl; Fig. 1) was synthesized by ENDOTHERM GmbH (Saarbruecken, Germany) according to Harrison et al. (2003). Identity and puritiy were proven by NMR (Table 3) and HPLC, respectively, in comparison with the original compound.

2.2. Buffers and cell culture medium for stability studies

For stability studies different HBSS (Hank's balanced salt solution) buffers and diluted McIlvain buffer were used.

The basic compositions of HBSS buffers were: 137.0 mM NaCl, 5.36 mM KCl, 4.26 mM $NaHCO_3$, 0.18 mM $Na_2HPO_4 \times 7H_2O$, 0.44 mM KH_2PO_4, 5.55 mM Glucose, 0.13 mM $CaCl_2 \times 2H_2O$, 0.05 mM $MgCl_2 \times 6H_2O$, 0.04 mM $MgSO_4 \times 7H_2O$. For the adjustment of the appropriate pH values in HBSS buffers the buffering substances were exchanged as follows: pH 7.4 and 7.0: 10.0 mM HEPES (*N*-[2-hydroxyethyl]piperazine-*N*′-[2-ethanesulfonic acid]), pH 6.0: 10.0 mM MES (2-morpholinoethanesulfonic acid), pH 4.0 and 5.0: 10.0 mM sodium acetate. pH values were adjusted with 1 M NaOH or 1 M HCl, respectively.

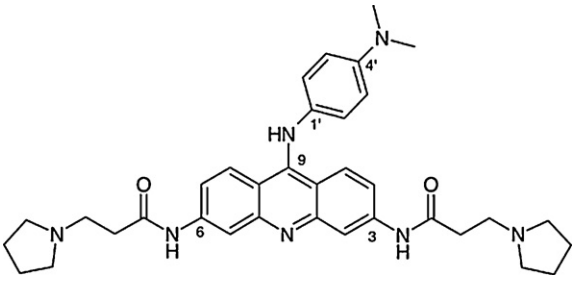

Fig. 1. Structure of BRACO19 ((9-[4-(*N*,*N*-dimethylamino)phenylamino]-3,6-bis(3-pyrrolodino-propionamido) acridine).

Diluted McIlvain buffer contained 50 mM citric acid and 1.4 mM Na_2HPO_4. The pH was 2.8. Phosphate buffer was composed of 5 mM KH_2PO_4 and the pH was adjusted with NaOH to pH 7.4.

RPMI cell culture medium was purchased from PAA Laboratories GmbH (Pasching, Austria) and supplemented with 10% FCS (Sigma–Aldrich Chemie GmbH, Taufkirchen, Germany). The pH of the cell culture medium was 7.5.

2.3. HPLC-DAD analysis of BRACO19 and decomposition products

BRACO19 was analyzed by reversed phase HPLC using an isocratic Dionex HPLC system consisting of an ASI 100 automated sample injector with adjustable temperature, UVD 340U diode array detector (DAD) and P680 pump with Chromeleon® software (version 6.60 SP1 build 1449) (Dionex, Idstein, Germany).

We used a Gemini® RP-18 column/150 × 4.6 mm/5 μm/110 Å (Phenomenex, Aschaffenburg, Germany). The mobile phase was composed of 80:20 (v/v) methanol:borate buffer pH 10.0 (100 mM). At a flow rate of 0.6 ml/min the retention time of BRACO19 was 8.9 ± 0.2 min. The wavelength of the detector was set at 268 nm. The detection and quantification limit of BRACO19 were 0.010 and 0.025 μg/ml, respectively. Quantification was linear in the range from 0.025 to 12 μg/ml.

2.4. Decomposition experiments

All decomposition experiments were performed with the HPLC-DAD system described above in HPLC brown glass vials (hydrolysis grade 1; CS-Chromatography, Langerwehe, Germany). Decomposition experiments over 7 h were performed at 37° with HBSS buffer of different pH values and diluted McIlvain buffer of pH 2.8. The influence of temperature on BRACO19 decomposition was assessed at 4 °C in comparison to the decomposition at 37 °C in HBSS buffer pH 7.4. BRACO19 was dissolved at a concentration of 12 μg/ml in each respective buffer. 20 μl samples were drawn every 45 min for 7 h and analyzed by HPLC as described above. Each experiment was done in triplicate.

Long-term decomposition experiments were performed for 4 days in HBSS buffer pH 7.4, phosphate buffer pH 7.4 and RPMI cell culture medium containing 10% FCS (pH 7.5), respectively. The concentration of BRACO19 was 12 μg/ml and the temperature was set to 37 °C. Samples were drawn every 2.54 h. All experiments were performed in triplicate.

UV spectra of degradation products were recorded with the DAD detector during these long-term experiments.

The decomposition of BRACO19 in different media was described mathematically by assuming first order kinetics. A non-weighted curve fitting was performed using the software Origin (Version 7.5, OriginLab Corp., Northampton, MA, USA) according to the formula:

$$A = A_0 e^{(-kt)} \quad (1)$$

where A is the amount of BRACO19 (in %) at time point t_i, A_0 the amount at time point $t = 0$, k the rate constant (in h^{-1}) and t is the time (in h).

2.5. Decomposition of BRACO19 for structural analysis of decomposition products by LC/MS and NMR

For the analysis of the decomposition products by LC/MS and NMR BRACO19 was dissolved in phosphate buffer pH 7.4 at a concentration of 55 μg/ml. The solution was kept at room temperature for 14 days (~20 °C). The longer decomposition time was necessary to obtain larger amounts of secondary decomposition products. Decomposition was confirmed by HPLC. LC/MS and NMR analyses were performed with the mixture of decomposition products without isolation and purification of degradation products.

2.6. LC/MS analysis of decomposition products

The Surveyor®-LC-system consisted of a pump, an autosampler, and a PDA detector. Mass spectrometry was performed on a TSQ® Quantum (Thermo Electron Corporation, Dreieich, Germany). The triple quadrupole mass spectrometer was equipped with an electrospray interface (ESI). The system was operated by the standard software Finnigan™ Xcalibur® (Thermo Electron Corporation).

A RP C18 NUCLEODUR® 100-5 (125 mm × 3 mm) column (Macherey-Nagel GmbH, Duehren, Germany) was used as stationary phase. The solvent system consisted of 0.1% formic acid (A) and 0.1% formic acid in methanol (B). Injection volume was 20 μl and flow rate was set to 350 μl/min. From 0 to 10 min the percentage of B in the mixture was increased from 20 to 100% and kept at 100% for 3 min. From 13 to 15 min the percentage of B was decreased to the initial 20%. MS analysis was carried out at a spray voltage of 4200 V, a capillary temperature of 350 °C and a source CID of 10 V. The polarity of the mass spectrometer was positive and as scan mode a full scan from 100 to 800 *m/z* was chosen as first scan event.

In a second scan event, the most intense ion determined in scan event one was collided with argon, at a collision gas pressure of 0.9 Pa and a collision energy of 35 V. The resulting fragments were recorded in MS/MS mode.

2.7. NMR analysis of BRACO 19 and decomposition products

In NMR analysis the ^{1}H NMR spectra of (a) the free base of BRACO19 and (b) the decomposition products were compared. For this purpose aqueous solutions of both were lyophilized and redissolved in CD_3OD. The ^{1}H NMR spectra (500 MHz) of (a) and (b) were recorded at 298 K on a Bruker DRX500 spectrometer using the standard pulse program zg30. Chemical shifts are given in parts per million (ppm) on the δ scale referenced to the solvent peak at 3.30 ppm.

2.8. TRAP assay

The *T*elomeric *R*epeat *A*mplification *P*rotocol (TRAP) assay was performed according to the instructions of the $TRAP_{EZE}$® Telomerase Detection Kit (Chemicon International, Temecula, CA, USA), a modified version of the TRAP assay originally developed by Kim et al. (1994) and Kim and Wu (1997). Fifty nanograms of a protein extract from lysed A549 lung cancer cells was used per reaction. Decomposition products were obtained from a sample of the solution used for LC/MS and NMR analysis. The absence of intact BRACO19 in the mixture of decomposition products was verified by the HPLC-DAD method described above. The concentrations of BRACO19 and of decomposition products were 2.0, 1.0, 0.5, 0.25, and 0.1 μM. The concentrations refer to the initial BRACO19 concentration. One micromolar BRACO19 and decomposition products,

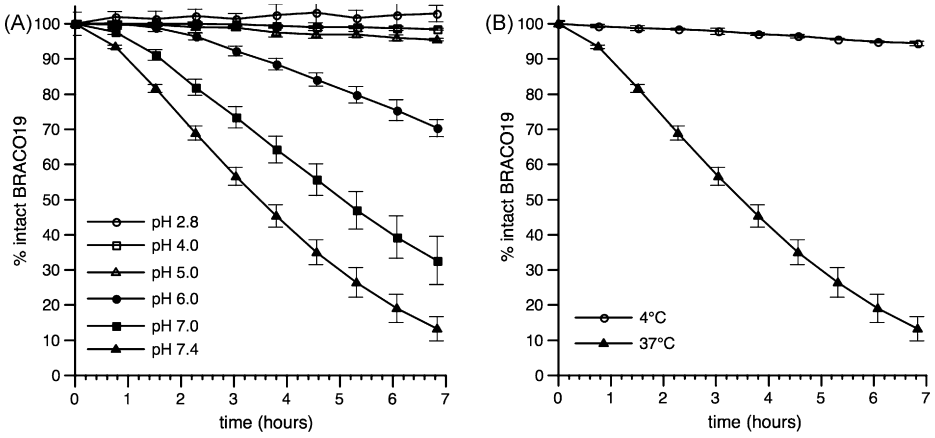

Fig. 2. (A) Stability of BRACO19 at 37 °C in HBSS buffers of different pH values (pH 7.4–4) and McIlvain buffer (pH 2.8); (B) Stability of BRACO19 in HBSS buffer pH 7.4 at 4 °C and 37 °C.

respectively, were added to the control template TSR8. Cell lysis buffer was included as negative control. TRAP products were separated on a 12.5% non-denaturating polyacrylamide gel. DNA fragments were visualized after SYBR® Green I staining (Molecular Probes, Eugene, OR, USA) with the Gel Doc™ 2000 Gel Documentation System from BioRad (BioRad Laboratories GmbH, Munich, Germany).

3. Results

3.1. Stability experiments

The stability of BRACO19 in solution was found to be dependent on pH and temperature. As can be seen in Fig. 2A at 37 °C the stability of BRACO19 increased gradually with decreasing pH of the HBSS buffer. It was least stable at pH 7.4 while at pH 2.8 (McIlvain buffer) no decomposition occurred. Also, when BRACO19 was dissolved in HBSS buffer pH 7.4 and analyzed at 4 and 37 °C the decomposition at 4 °C was considerably slower than at 37 °C (Fig. 2B). An exchange of the brown glass HPLC vials with clear glass vials or polypropylene vials did not affect the results of the stability assays (data not shown).

In long-term experiments the type of dissolution medium exerted a less important influence on the stability of BRACO19 than the variation of pH or temperature. As can be seen in Fig. 3 and Table 1 the decomposition was fastest in HBSS buffer pH 7.4. In standard phosphate buffer and RPMI cell culture medium the stability was only slightly better. The half-life in HBSS buffer was about 2.9 h. In phosphate buffer and RPMI cell culture medium half-lives were about 4 and 4.4 h, respectively. Total decomposition occurred within 1 day in all solutions at 37 °C. Four decomposition products (termed Decomp1–4) were identified during these long-term experiments in HBSS buffer and phosphate buffer. Their retention times in the HPLC-DAD system are given in Table 2. The decomposition products could

Table 1
Rate constants, half-lifes ($t_{1/2}$) (± standard error) and R^2s of fits for the decomposition of BRACO19 in HBSS buffer, phosphate buffer and RPMI cell culture medium at 37 °C

Medium	Rate constant (h^{-1})	$t_{1/2}$ (h)	R^2 of fit
HBSS buffer pH 7.4	0.303 ± 0.026	2.9 ± 0.17	0.986
Phosphate buffer pH 7.4	0.174 ± 0.012	4.0 ± 0.27	0.985
RPMI cell culture medium pH 7.5	0.157 ± 0.016	4.4 ± 0.45	0.967

Table 2
Retention times of BRACO19s decomposition products after decomposition in HBSS buffer pH 7.4 (average ± standard deviation)

	Retention time (min)
BRACO19	8.20 ± 0.20
Decomp1	6.71 ± 0.02
Decomp2	5.16 ± 0.01
Decomp3	5.38 ± 0.02
Decomp4	4.44 ± 0.02

For HPLC-DAD parameters see Section 2.

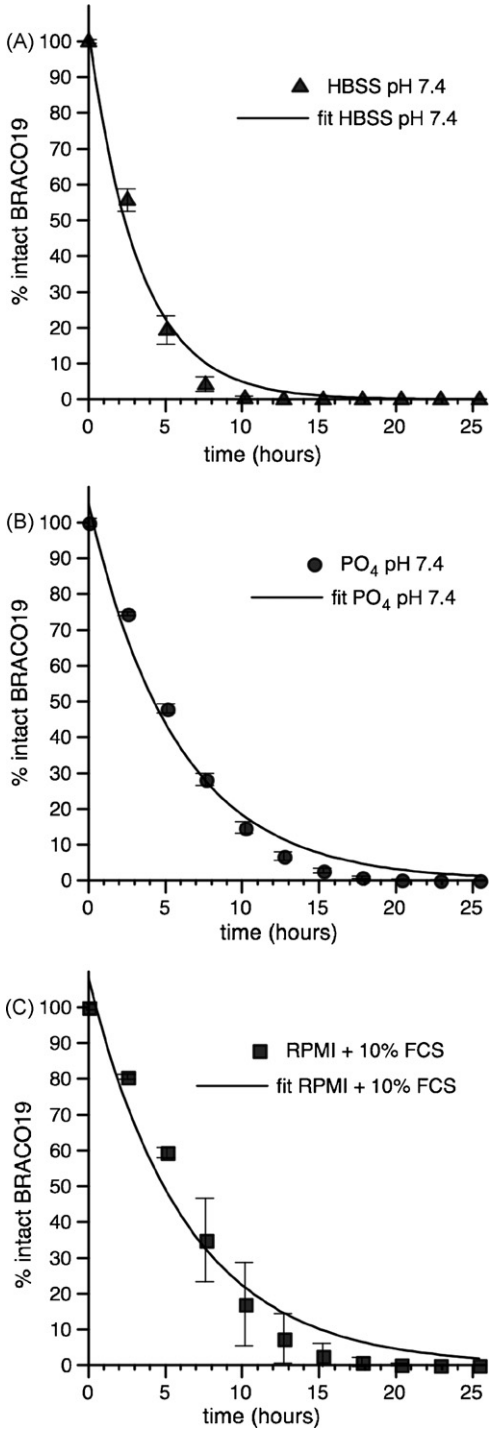

Fig. 3. Decomposition of BRACO19 in HBSS buffer pH 7.4 (A), phosphate buffer pH 7.4 (B) and RPMI cell culture medium pH 7.5 (C). Curves were fitted according to formula 1 assuming first order kinetics. Fit results are given in Table 1.

easily be distinguished by their UV spectra and were the same in HBSS buffer and phosphate buffer (Fig. 4). In cell culture medium only Decomp2 could be detected under the given conditions (data not shown). As can be seen in Fig. 5 Decomp1 and Decomp2 appeared first but were also instable. Their decay curves resemble a Bateman-function as seen in pharmacokinet-

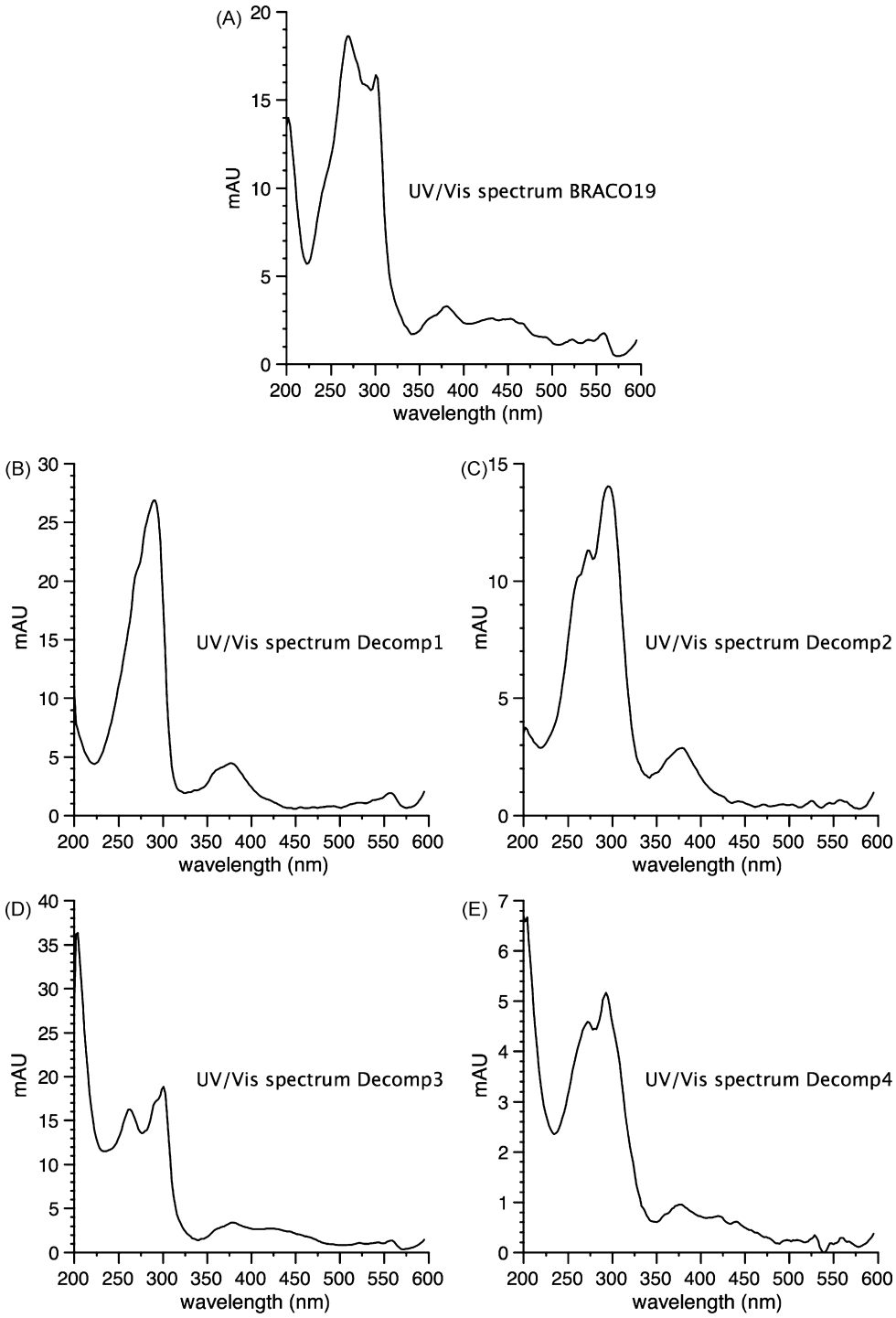

Fig. 4. UV/Vis spectra of BRACO19 and its decomposition products in the range from 200 to 600 nm. The spectra were obtained during long-term HPLC-DAD analysis with methanol: borate buffer pH 10 (80:20) as mobile phase. A: BRACO19; B: Decomp1; C: Decomp2; D: Decomp3; E: Decomp4. Spectra are corrected for spectra of mobile phase.

ics after oral administration of a drug. Decomp3 and Decomp4 appeared much slower and showed a steady increase over time and might be the decomposition products of Decomp1 and Decomp2. However, since the exact structures and concentrations of the decomposition products were unknown a calculation of kinetic parameters was not possible.

3.2. LC/MS and NMR analysis

The analysis of the decomposition mixture by LC/MS resulted in the discovery of a molecule with a mass (*m*/*z*) of 144.2, which corresponds to the mass of the $[M+H]^+$ of 3-pyrrolidino propionic acid (structure **2** in Fig. 6), i.e. the residue

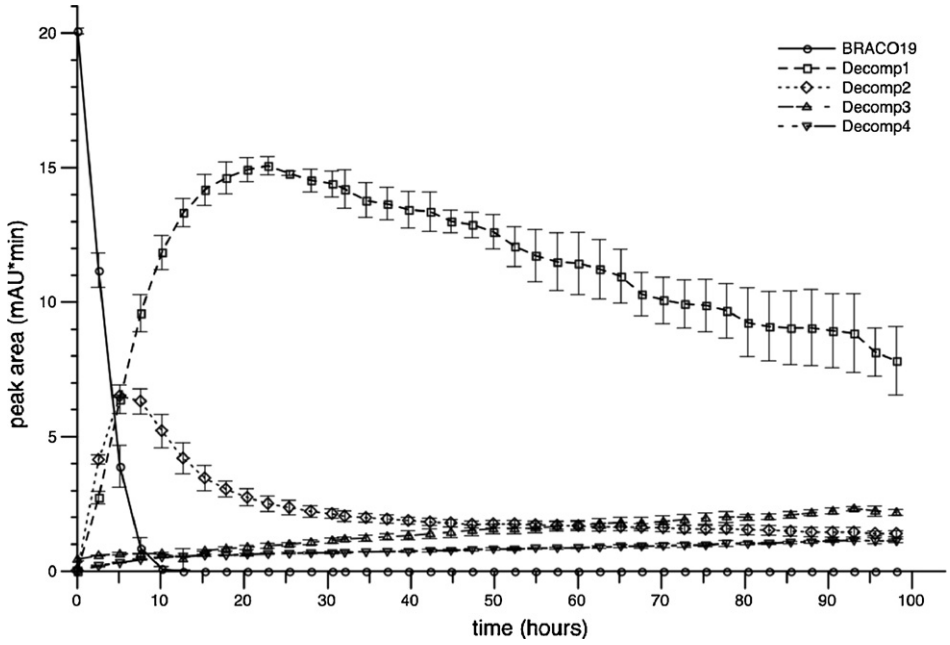

Fig. 5. Decomposition of BRACO19 at 37 °C in HBSS buffer pH 7.4 over 4 days as determined by HPLC-DAD analysis. Decomp1 and Decomp2 are the first decomposition products of BRACO19 while Decomp3 and Decomp4 appear to be the decomposition products of Decomp1 and Decomp2. Each data point represents mean ± standard deviation of 3 independent measurements.

of the amide groups in position 3 and 6 of BRACO19. Thus, hydrolysis of these amides seems to be likely. However, no molecule ions were found that would match the corresponding reaction products (structures **3** and **4** in Fig. 6). Instead, molecule ions with masses of 567.6, 442.5 and 317.3 were detected. These masses correspond to the $[M+H]^+$ of structures **5**, **6**, and **7**, respectively, indicating a deamination in 4′ position, i.e. an exchange of the dimethyl amino group for a hydroxyl group. In MS/MS scans a fragment with the mass of 84.2 was found for structures **2**, **5**, and **6** but not for structure **7**. This fragment matches the structure of *N*-methyl pyrrolidine and confirms the hypothesis of a hydrolysis of the amide groups.

The NMR analyses of the decomposition products confirm the findings of LC/MS analysis. The results of the measurements are given in Table 3. In the aromatic part of the ^{1}H NMR spectrum signals of two compounds (i) and (ii) can be found in a ratio of 5 to 1. The data of the major compound (i) are close to those of BRACO19 but lack signals for a dimethyl amino group in the aliphatic part of the spectrum, indicating the presence of a hydroxyl instead of the dimethyl amino group. The data of (i) are in good accordance with structure **5**. Investigation of the NMR spectral data of the minor compound (ii) showed that in contrast to BRACO19 the signals of the outer rings of the acridine system are not identical anymore. The difference of the chemical shifts of both benzene subunits (δ 8.33, 7.99, 7,21 vs. 7.71, 6.69, 6.65) suggests that the molecule has only one 3-pyrrolidino propionic acid group. Correspondingly, the aliphatic part of the ^{1}H NMR spectrum reveals only signals for one 3-pyrrolidino propionic acid moiety. This together with the fact that the dimethyl amino group is absent leads to structure **6** for compound (ii).

The solution must also contain free 3-pyrrolidino propionic acid (structure **2**), since the values for the integrals of the 3-pyrrolidino propionic acid groups are bigger than required for pure compound (i) and (ii).

3.3. TRAP assay

Decomposed BRACO19 (1 and 2 μM) was still able to reduce the number and intensities of the bands representing the "telomere ladder" (Fig. 7, D1–D5). When compared to intact BRACO19 (Fig. 7, B1–B5) the decomposition products

Table 3
^{1}H NMR spectral data of compounds BRACO 19, (i) and (ii)

	BRACO 19 δ_H (ppm)	(i) δ_H (ppm)	(ii) δ_H (ppm)
1	7.91 brd (J = 9)	7.99 brd (J = 9)	7.71 brd (J = 9)
2	7.20 brd (J = 9)	7.25 brd	6.69 brd (J = 9)
4	8.09 brs	8.39 brs	6.65 brs
5	8.09 brs	8.39 brs	8.33 brs
7	7.20 brd (J = 9)	7.25 brd (J = 9)	7.21 brd (J = 9)
8	7.91 brd (J = 9)	7.99 brd (J = 9)	7.99 brd (J = 9)
2′, **6′**	6.80 *d* (J = 8.5)	7.13 d (J = 8.5)	7.13 d (J = 8.5)
3′, **5′**	6.90 d (J = 8.5)	6.89 d (J = 8.5)	6.89 d (J = 8.5)
1″	2.88 m (2H)	3.07 m	3.07 m
2″	2.64 m (2H)	2.79 m	2.79 m
3″, **6″**	2.66 m (4H)	2.84 m	2.84 m
4″, **5″**	1.84 m (4H)	1.91 m	1.91 m
NCH_3	2.88 s (6H)	–	–

Coupling constants are given in parentheses. s: singlet; d: douplet; brs: broad singlet; brd: broad douplet. Signals indicated as m were unresolved or overlapped multiplets.

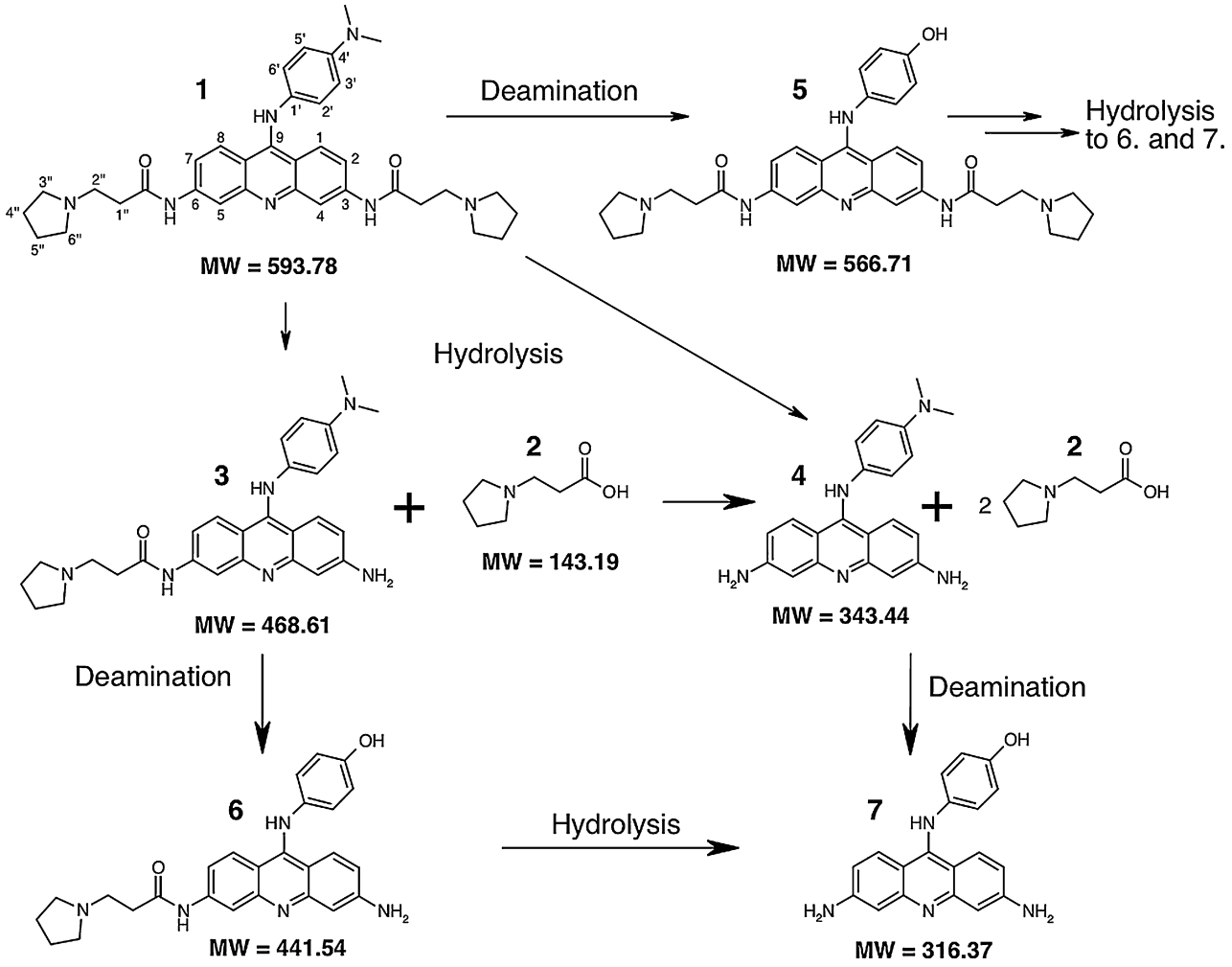

Fig. 6. The suggested reaction scheme for the decomposition of BRACO19 (**1** = BRACO19). The most important reactions for the decomposition seem to be the hydrolysis of the amide groups in position 3 and 9 and the deamination of the dimethyl amine group in position 4′ of the phenyl ring.

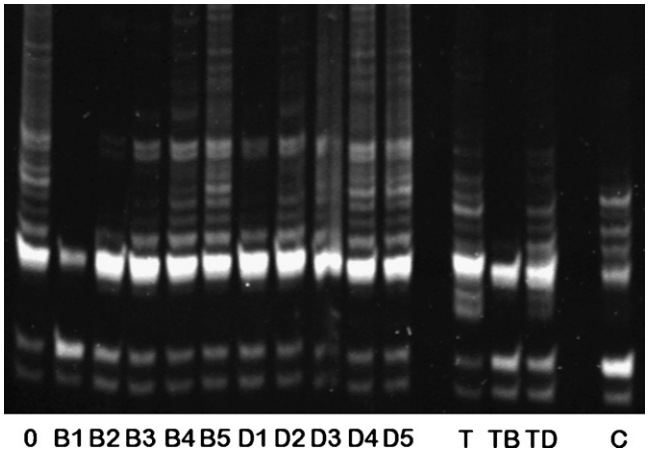

Fig. 7. The TRAP assay shows the effects of BRACO19 and its decomposition products on telomerase activity. The assay was performed with the same material that has been used for LC/MS and NMR analysis. 0 is the positive control; B1–B5: BRACO19 2, 1, 0.5, 0.25 and 0.1 μM; D1–D5: mixture of decomposition products 2, 1, 0.5, 0.25 and 0.1 μM (referred to initial BRACO19 concentrations); T: TSR8 internal standard; TB: TSR8 internal standard with 1 μM BRACO19; TD: TSR8 internal standard with 1 μM decomposition products; C: negative control (lysis buffer). This figure is representative for two TRAP assays that were performed with BRACO19 and its decomposition products.

showed a reduced inhibitory effect. Inhibition of telomerase with BRACO19 at a concentration of 0.25 μM clearly reduced the band intensities of the telomerase products. At 0.5 μM the length of the telomere ladder was considerably shorter. For the decomposition products the same effects were observed at 1 and 2 μM, respectively, demonstrating their reduced inhibitory potential. Both, BRACO19 and the mixture of decomposition products, influenced the amplification of the TSR8 internal standard. For BRACO19 no bands could be found. The decomposition products reduced the band intensities slightly (Fig. 7T, TB and TD). The bands in the control Lane (Fig. 7C) are most likely due to primer–dimer artifacts. Fig. 7 is representative for two TRAP assays that were performed with BRACO19 and its decomposition products.

4. Discussion

Our experiments demonstrate that the stability of BRACO19 considerably depends on pH and temperature of standard buffers used in biological test systems. At physiological pH BRACO19 decomposed in simple phosphate buffer as well as in more complex cell culture medium. One important mechanism of this

decomposition seems to be a hydrolysis of the amide bonds in position 3 and 6 of the acridine part of the molecule as has been shown by LC/MS and NMR analysis. The decomposition is pH dependent and can be approximated by first-order kinetics. The primary decomposition products were also unstable and decomposed further into other products. However, since the exact structures and concentrations of the decomposition products are unknown a determination of kinetic parameters was not feasible. Derivatives of 9-aminoacridine are described to be prone to hydrolysis in position 9 resulting in acridones (Goodell et al., 2006). In our studies such products could not be found. Instead, a deamination in 4′-position of the phenyl residue seems to be more likely.

BRACO19 has been described as the prototype of a new generation of aminoacridine based anti-cancer drugs that act as telomerase inhibitors by G-quadruplex stabilization in telomeres. A modification of the acridine ring in position 3 and 6 with an aminoalkylamide side chain containing a basic heterocycle (i.e. the pyrrolidine ring in BRACO19) is essential to obtain stable complexes between the quadruplex structures and the drug molecule. The heterocycle is protonated under physiological conditions and thus positively charged. The side chains are directed towards the G-quadruplex grooves where they can interact with the negatively charged phosphate backbones of the DNA (Read et al., 1999; Harrison et al., 2003, 2004). Moore et al. have shown that 9-aminoacridine derivatives without these side chains in position 3 and 6 form only very weak complexes and are not able to inhibit telomerase activity (Moore et al., 2006). Our results show that the decomposition, i.e. the hydrolysis of the side chains and the deamination in 4′-position strongly influences the inhibitory effect of BRACO19. In the TRAP assay a significant reduction of telomerase activity only occurs at the highest concentration of decomposition products derived from 2 μM BRACO19 (Fig. 7D1). The interference with the amplification of the TSR8 standard is not as pronounced as with BRACO19 as can be seen in Fig. 7 when lines T, TB and TD are compared. TSR8 is an oligonucleotide composed of the TS-primer + 8 telomeric repeats. In the TRAP assay it is normally used as a quantitation control in the absence of telomerase. In a previous study we were able to show that BRACO19 strongly interferes with the amplification of the TSR8 oligonucleotide during PCR (Piotrowska et al., 2005). The mechanism for this interference is the formation and stabilization of G-quadruplexes within TSR8, which prevents a proper PCR reaction (De Cian et al., 2007). The reduced inhibition of the amplification of TSR8 by the decomposition products indicates that the affinity of the decomposition products to G-quadruplex structures is strongly reduced. Whether the remaining inhibitory effect can be attributed to one of the decomposition products alone or to all of them will be the matter of further studies. A reasonable order for inhibitory potential can be established by following the degree of hydrolysis of the pyrrolidino-propionamido groups: structure **5** > structure **6** > structure **7** (Fig. 6).

The instability of BRACO19 under physiological conditions will cause some problems when the agent is used in biological test systems. Concerning the animal studies that were performed so far (Burger et al., 2005) it would be interesting to gain more knowledge about the metabolism of BRACO19, i.e. if the effects that have been described are really due to BRACO19 or one of its decomposition products.

In conclusion, G-quadruplex stabilizing substances from the class of alkylamidoacridines like BRACO19 appear to be promising new drug molecules for the treatment of cancer by telomerase inhibition and telomere dysregulation.

However, the results presented in this study show that this class of compounds may face stability problems during the preparation of dosage forms, their storage and after application. This might have serious consequences for the therapeutical success. Any new drug candidate should be submitted to thorough stability investigations prior to in vitro and in vivo tests. We have shown previously that BRACO19 is also a problematic substance from the biopharmaceutical point of view (Taetz et al., 2006). Since research in this field is continued and new substances based on the alkylamidoacridine structure are being developed (Martins et al., 2007) it can be concluded that compounds like BRACO19 will require either further chemical modifications or a suitable formulation and delivery strategy to (i) improve their biopharmaceutical properties and (ii) reduce stability problems.

Acknowledgements

This project is financially supported by Deutsche Krebshilfe e.V., Bonn, Germany (Project No.: 10-2035-Kl I) and the Robert Bosch Foundation, Stuttgart, Germany.

References

Blackburn, E.H., 2005. Telomeres and telomerase: their mechanisms of action and the effects of altering their functions. FEBS Lett. 579, 859.

Burger, A.M., Dai, F., Schultes, C.M., Reszka, A.P., Moore, M.J., Double, J.A., Neidle, S., 2005. The G-quadruplex-interactive molecule BRACO-19 inhibits tumor growth, consistent with telomere targeting and interference with telomerase function. Cancer Res. 65, 1489–1496.

Cuesta, J., Read, M.A., Neidle, S., 2003. The design of G-quadruplex ligands as telomerase inhibitors. Mini Rev. Med. Chem. 3, 11–21.

De Cian, A., Cristofari, G., Reichenbach, P., De Lemos, E., Monchaud, D., Teulade-Fichou, M.P., Shin-Ya, K., Lacroix, L., Lingner, J., Mergny, J.L., 2007. Reevaluation of telomerase inhibition by quadruplex ligands and their mechanisms of action. Proc. Natl. Acad. Sci. U.S.A. 104, 17347–17352.

Goodell, J., Svensson, B., Ferguson, D., 2006. Spectrophotometric determination and computational evaluation of the rates of hydrolysis of 9-amino-substituted acridines. J. Chem. Inf. Model. 46, 876–883.

Gowan, S.M., Harrison, J.R., Patterson, L., Valenti, M., Read, M.A., Neidle, S., Kelland, L.R., 2002. A G-quadruplex-interactive potent small-molecule inhibitor of telomerase exhibiting in vitro and in vivo antitumor activity. Mol. Pharmacol. 61, 1154–1162.

Harrison, R.J., Cuesta, J., Chessari, G., Read, M.A., Basra, S.K., Reszka, A.P., Morrell, J., Gowan, S.M., Incles, C.M., Tanious, F.A., Wilson, W.D., Kelland, L.R., Neidle, S., 2003. Trisubstituted acridine derivatives as potent and selective telomerase inhibitors. J. Med. Chem. 46, 4463–4476.

Harrison, R.J., Reszka, A.P., Haider, S.M., Romagnoli, B., Morrell, J., Read, M.A., Gowan, S.M., Incles, C.M., Kelland, L.R., Neidle, S., 2004. Evaluation of by disubstituted acridone derivatives as telomerase inhibitors: the importance of G-quadruplex binding. Bioorg. Med. Chem. Lett. 14, 5845–5849.

Kim, N.W., Piatyszek, M.A., Prowse, K.R., Harley, C.B., West, M.D., Ho, P.L., Coviello, G.M., Wright, W.E., Weinrich, S.L., Shay, J.W., 1994. Specific association of human telomerase activity with immortal cells and cancer. Science 266, 2011–2015.

Kim, N.W., Wu, F., 1997. Advances in quantification and characterization of telomerase activity by the telomeric repeat amplification protocol (TRAP). Nucleic Acids Res. 25, 2595–2597.

Martins, C., Gunaratnam, M., Stuart, J., Makwana, V., Greciano, O., Reszka, A.P., Kelland, L.R., Neidle, S., 2007. Structure-based design of benzylamino-acridine compounds as G-quadruplex DNA telomere targeting agents. Bioorg. Med. Chem. Lett. 17, 2293–2298.

Moore, M.J., Schultes, C.M., Cuesta, J., Cuenca, F., Gunaratnam, M., Tanious, F.A., Wilson, W.D., Neidle, S., 2006. Trisubstituted acridines as G-quadruplex telomere targeting agents. Effects of extensions of the 3,6- and 9-side chains on quadruplex binding, telomerase activity, and cell proliferation. J. Med. Chem. 49, 582–599.

Pendino, F., Tarkanyi, I., Dudognon, C., Hillion, J., Lanotte, M., Aradi, J., Ségal-Bendirdjian, E., 2006. Telomeres and telomerase: pharmacological targets for new anticancer strategies? Curr. Cancer Drug Targets 6, 147–180.

Piotrowska, K., Kleideiter, E., Mürdter, T.E., Taetz, S., Baldes, C., Schaefer, U., Lehr, C.M., Klotz, U., 2005. Optimization of the TRAP assay to evaluate specificity of telomerase inhibitors. Lab. Invest. 85, 1565–1569.

Read, M.A., Wood, A.A., Harrison, J.R., Gowan, S.M., Kelland, L.R., Dosanjh, H.S., Neidle, S., 1999. Molecular modeling studies on G-quadruplex complexes of telomerase inhibitors: structure-activity relationships. J. Med. Chem. 42, 4538–4546.

Riou, J.F., 2004. G-quadruplex interacting agents targeting the telomeric G-overhang are more than simple telomerase inhibitors. Curr. Med. Chem. Anticancer Agents 4, 439–443.

Shay, J.W., Wright, W.E., 2004. Senescence and immortalization: role of telomeres and telomerase. Carcinogenesis 26, 867–874.

Shay, J.W., Wright, W.E., 2006. Telomerase therapeutics for cancer: challenges and new directions. Nat. Rev. Drug Discov. 5, 577–584.

Taetz, S., Baldes, C., Mürdter, T.E., Kleideiter, E., Piotrowska, K., Bock, U., Haltner-Ukomadu, E., Mueller, J., Huwer, H., Schaefer, U.F., Klotz, U., Lehr, C.M., 2006. Biopharmaceutical characterization of the telomerase inhibitor BRACO19. Pharm. Res. 23, 1031–1037.